Werber, M. M., Szent-Gyorgyi, A. G., & Fasman, G. D. (1972) *Biochemistry 11*, 2872.
Werber, M. M., Oplatka, A. & Danchin, A. (1974) *Biochemistry 13*, 2683.
Yoshikawa, M., Kato, T., & Takenishi, T. (1967) *Tetrahedron Lett.*, 5065.
Yount, R. G., Babcock, D., Ballantyne, W., & Ojala, D. (1971) *Biochemistry 10*, 2484.

Kinetic Mechanisms of Two NAD:Arginine ADP-Ribosyltransferases: The Soluble, Salt-Stimulated Transferase from Turkey Erythrocytes and Choleragen, a Toxin from *Vibrio cholerae*

James C. Osborne, Jr.,*,‡ Sally J. Stanley,§ and Joel Moss§
Molecular Disease Branch and Laboratory of Cellular Metabolism, National Heart, Lung, and Blood Institute, National Institutes of Health, Bethesda, Maryland 20205
Received November 28, 1984

ABSTRACT: A subunit of choleragen and an erythrocyte ADP-ribosyltransferase catalyze the transfer of ADP-ribose from NAD to proteins and low molecular weight guanidino compounds such as arginine. These enzymes also catalyze the hydrolysis of NAD to nicotinamide and ADP-ribose. The kinetic mechanism for both transferases was investigated in the presence and absence of the product inhibitor nicotinamide by using agmatine as the acceptor molecule. To obtain accurate estimates of kinetic parameters, the transferase and glycohydrolase reactions were monitored simultaneously by using [*adenine*-2,8-^{3}H]NAD and [*carbonyl*-^{14}C]NAD as tracer compounds. Under optimal conditions for the transferase assay, NAD hydrolysis occurred at <5% of the V_{max} for ADP-ribosylation; at subsaturating agmatine concentrations, the ratio of NAD hydrolysis to ADP-ribosylation was significantly higher. Binding of either NAD or agmatine resulted in a greater than 70% decrease in affinity for the second substrate. All data were consistent with a rapid equilibrium random sequential mechanism for both enzymes.

ADP-ribosylation is a covalent modification in which the ADP-ribose moiety of NAD is transferred to specific proteins (reaction 1) (Hayaishi & Ueda, 1977; Vaughan & Moss, 1982; Pekala & Moss, 1983). Several amino acids can serve as ADP-ribose acceptors; among these are arginine (Goff, 1974; Moss & Vaughan, 1977, 1978; Moss & Richardson, 1978), glutamate (Riquelme et al., 1979; Burzio et al., 1979; Ogata et al., 1980a,b), asparagine (Manning et al., 1984), and diphthamide (Van Ness et al., 1980a,b), a posttranslationally modified histidine residue. These ADP-ribosyltransferases also catalyze the hydrolysis of NAD to ADP-ribose and nicotinamide (reaction 2) (Moss & Vaughan, 1978; Kandel et al., 1974; Moss et al., 1976, 1983; Ueda et al., 1975; Katada et al., 1983). The presence of this abortive reaction indicates that the transferases are capable of activating the ribosyl–nicotinamide bond in the absence of an amino acid or protein acceptor. It is possible that binding of the ADP-ribose acceptor requires the initial binding of NAD (ordered sequential mechanism) or that, in fact, both substrates bind independently (random sequential mechanism). Chung & Collier (1977) have investigated the kinetics of interaction of NAD and the ADP-ribose acceptor with diphtheria toxin. This bacterial toxin is a member of one class of ADP-ribosyltransferases that catalyzes the ADP-ribosylation of a modified histidine residue in elongation factor II (Van Ness et al., 1980a,b), thereby inhibiting protein synthesis (Chung & Collier, 1977). These investigators presented a model in which NAD binding must precede the binding of elongation factor II (EF-2) (reactions 3a,b) (Chung & Collier, 1977). The formation of a ternary complex, i.e., enzyme–NAD–acceptor, is supported by the finding that all ADP-ribosyltransferases appear to be stereospecific (Ferro & Oppenheimer, 1978; Oppenheimer, 1978; Moss et al., 1979a,b; Oppenheimer & Bodley, 1981); the enzymes use β-NAD as a substrate and, in the presence of an acceptor, form the α-anomeric product.

$$\text{NAD} + \text{protein} \rightarrow \text{ADP-ribose protein} + \text{nicotinamide} + \text{H}^+ \quad (1a)$$

$$\text{NAD} + \text{amino acid} \rightarrow \text{ADP-ribose–amino acid} + \text{nicotinamide} + \text{H}^+ \quad (1b)$$

$$\text{NAD} + \text{H}_2\text{O} \rightarrow \text{ADP-ribose} + \text{nicotinamide} + \text{H}^+ \quad (2)$$

$$\text{enzyme} + \text{NAD} \rightleftharpoons \text{enzyme–NAD} \quad (3a)$$

$$\text{enzyme–NAD} + \text{EF-2} \rightleftharpoons \text{enzyme–NAD–EF-2} \rightarrow \text{products} \quad (3b)$$

A subclass of ADP-ribosyltransferases uses free arginine, in addition to proteins, as ADP-ribose acceptors (Moss & Vaughan, 1977, 1978; Moss & Richardson, 1978). Included in this group of enzymes are choleragen (cholera toxin) (Moss & Vaughan, 1977) and *Escherichia coli* heat-labile enterotoxin (Moss & Richardson, 1978), the bacterial toxins responsible for the activation of adenylate cyclase in animal cells (Moss & Vaughan, 1981), and erythrocyte NAD:arginine ADP-ribosyltransferases (Moss & Vaughan, 1978). We have examined the kinetics of the transferase reaction with two of these enzymes, cholera toxin (CT)[1] and erythrocyte transferase (ET). The studies support a model clearly different from that

‡ Molecular Disease Branch.
§ Laboratory of Cellular Metabolism.

[1] Abbreviations: CT, choleragen (cholera toxin); ET, erythrocyte transferase.

reported previously for diphtheria toxin (Chung & Collier, 1977).

Experimental Procedures

Materials

CT was purchased from Schwarz/Mann; agmatine, NAD, histone, lysolecithin, and ovalbumin were purchased from Sigma; [*adenine*-U-^{14}C]NAD (308 mCi/mmol), [*adenine*-2,8-^{3}H]NAD (25.7 Ci/mmol), and [*carbonyl*-^{14}C]NAD (57 mCi/mmol) were from Amersham; Triton X-100 was from Research Products International Corp.

Methods

ADP-Ribosyltransferase Assay. The ADP-ribosyltransferase assay for ET contained 50 mM potassium phosphate, pH 7.0, 1 mg/mL ovalbumin, [*adenine*-U-^{14}C]NAD (40 000 cpm), and the indicated concentrations of agmatine and NAD (total volume 0.3 mL). The reaction was initiated with transferase (0.131 milliunit) and incubated for 30 min at 30 °C; two 0.1-mL samples were then run over AG 1-X2 to resolve [*adenine*-U-^{14}C]ADP-ribose–agmatine from [*adenine*-U-^{14}C]NAD (Moss & Stanley, 1981). For CT, the standard assay contained 400 mM potassium phosphate, 20 mM dithiothreitol, 1 mg/mL ovalbumin, and [*adenine*-U-^{14}C]NAD (40 000 cpm); the reaction was initiated with CT (50 μg) which had been incubated with 20 mM dithiothreitol and 400 mM potassium phosphate, pH 7.0, for 40 min (Moss & Vaughan, 1977; Moss et al., 1976).

In the dual isotope experiments, a mixture of [*carbonyl*-^{14}C]NAD (25 000 cpm) and [*adenine*-2,8-^{3}H]NAD (15 000 cpm) was used in each assay. The reactants and products were separated by chromatography as follows: after assay, 0.1 mL (in duplicate) of each reaction mixture was layered on a 0.4 × 1.5 cm AG 1-X2 column and eluted with 5 mL of water into 10 mL of Hydrofluor scintillation fluid. Under these conditions, labeled NAD and ADP-ribose bind to the column whereas labeled [^{14}C]nicotinamide and [^{3}H]ADP-ribose–agmatine elute with the water washes. Transferase and total (i.e., transferase + glycohydrolase) velocities were computed respectively from the ^{3}H and ^{14}C radioactivity eluted from the column.

Enzyme Purification. ET was purified as described (Moss et al., 1980). Protein was determined by the method of Lowry et al. (1951) using bovine serum albumin as a standard.

Kinetic Analysis. Initial velocities as a function of variable substrate were obtained at several different fixed levels of the second substrate in the presence or absence of the inhibitor nicotinamide. The data were quantitatively analyzed in terms of rapid equilibrium and steady-state mechanisms by using classical double-reciprocal plots and replots of the primary data (Segel, 1975). In those cases where velocities were analyzed as the sum of glycohydrolase and transferase activities, the resulting double-reciprocal plots are difficult to evaluate by graphical methods (Segel, 1975). Kinetic parameters were quantified by using an on-line computer modeling program, MLAB, that allows comparison of experimental data to theoretical functions by the Marquardt–Levenberg curve-fitting method. Variable parameters in the theoretical function are adjusted so as to minimize the sum of squares of the differences between experimental and theoretical data. Theoretical equations were adapted from Segel (1975). Primary data were analyzed directly as velocity vs. substrate concentration profiles rather than as linear transformations in order to simplify data analysis. Final parameter values are given ±standard error. The experimental and theoretical curves are illustrated both in primary and in classical double-reciprocal form as a visual aid in mechanistic evaluations.

Results

Determination of K_m's for NAD in Reactions Catalyzed by CT and ET. In the absence of ADP-ribose acceptor, both CT (Figure 1b, inset) and ET (Figure 2b, inset) catalyzed the hydrolysis of NAD, with K_m's of 1.1 ± 0.1 mM and 7 ± 0.7 μM, respectively. Reactions were run for both proteins with variable NAD concentration using agmatine as the ADP-ribose acceptor. Initial analyses were consistent with a sequential rather than a ping-pong mechanism in that double-reciprocal plots with different fixed second substrate concentrations were linear and appeared to intersect at a single point. With both ET and CT, it appeared that when the data were plotted as $1/V$ vs. $1/[NAD]$ with variable [agmatine] or $1/V$ vs. $1/[agmatine]$ with variable [NAD] the lines intercepted below the abscissa (Figures 1 and 2). The combined data were thus inconsistent with an ordered mechanism in that the maximal velocity was dependent on the levels of both substrates and the apparent K_m for NAD increased with increasing fixed concentrations of agmatine.

Kinetic parameters were determined for the rapid equilibrium random mechanism directly from the primary data (eq 4). In this mechanism, the binding of one substrate alters

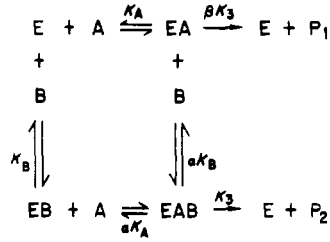

(4)

the binding of the other substrate by a factor α; if $\alpha < 1$, the affinity for the second substrate is increased, whereas if $\alpha > 1$ it is decreased. The apparent maximal velocity changes when either A or B serves as the variable substrate.

The unknowns in this analysis are the equilibrium constants for NAD and agmatine, the interaction parameter α, and the maximum velocity. The K_m for NAD was determined independently by measuring the glycohydrolase activity of both enzymes (insets to Figures 1b and 2b). The remaining kinetic parameters were then determined for both enzymes, as a function of varied NAD and agmatine concentrations, by a least-squares fit of initial velocity data to the above model. Our initial studies were performed with [*adenine*-U-^{14}C]NAD as a tracer, and thus, initial velocities corresponded only to the transfer reaction (eq 1). We found that the fit of the data for both enzymes was improved if a K_m for NAD different from that found for the glycohydrolase reaction was used in the data analysis. In view of this, initial velocities were measured by using a mixture of [*adenine*-2,8-^{3}H]NAD and [*carbonyl*-^{14}C]NAD in order to monitor, simultaneously, the transfer and glycohydrolase reactions. Use of the two labels allowed accurate estimates of maximal velocities for glycohydrolase and transfer reactions and the equilibrium constants for NAD and agmatine in the same experiment. The primary data, i.e., total velocity vs. substrate concentration, were fit to eq 5 in order to obtain the least-squares estimate of kinetic

$$V = V_{max}[A]/[K_A(1 + [B]/K_B)/(\beta + [B]/\alpha K_B) + [A](1 + [B]/\alpha K_B)/(\beta + [B]/\alpha K_A)] \quad (5)$$

parameters. In eq 5, A and B correspond to NAD and agmatine and K_A and K_B to their respective equilibrium constants, α is the factor by which binding of one substrate affects

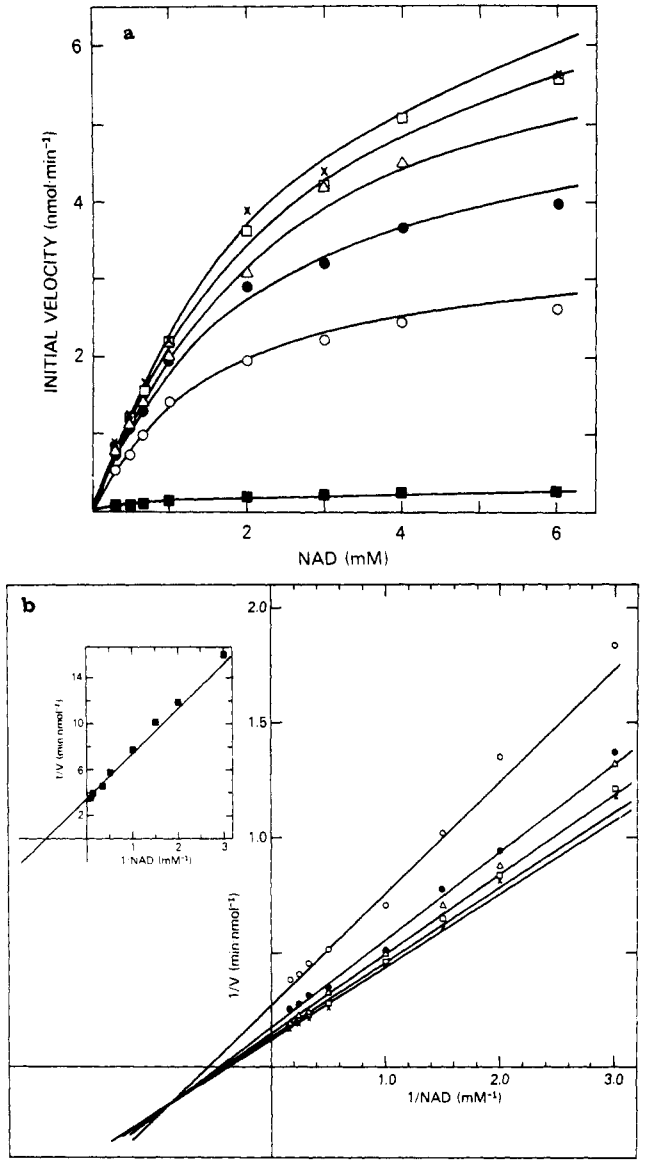

FIGURE 1: (a) Plot of the initial velocity of the conversion of NAD to products (both glycohydrolase and transfer reactions) vs. NAD concentration as obtained with cholera toxin. The closed squares correspond to the hydrolysis of NAD in the absence of acceptor. The remaining symbols correspond to reaction rates using agmatine as the ADP-ribose acceptor at the following concentrations: (○) 40, (●) 80, (△) 120, (□) 160, and (×) 200 mM. The standard reaction mix contained 400 mM potassium phosphate (pH 7.0), 20 mM dithiothreitol, and 1 mg/mL ovalbumin, and reactions were performed at 30 °C and initiated with cholera toxin (5 μg/assay). Hydrolysis and acceptor reaction rates were obtained for each assay by using a mixture of [*carbonyl*-^{14}C]NAD and [*adenine*-2,8-^{3}H]NAD as tracers. Additional experimental details are given under Methods. The solid lines correspond to the fit of the primary V vs. [S] data to the theoretical rapid equilibrium random sequential mechanism given under Results. Data in the presence and absence of acceptor were analyzed simultaneously. See text for details. (b) Double-reciprocal plot of the data in (a) using agmatine as the ADP-ribose acceptor. Symbols are the same as those in (a). Inset: Double-reciprocal plot of the data in (a) obtained in the absence of acceptor. The solid lines in the main figure and inset correspond to the fit of the experimental data to the rapid equilibrium random sequential mechanism given in the text.

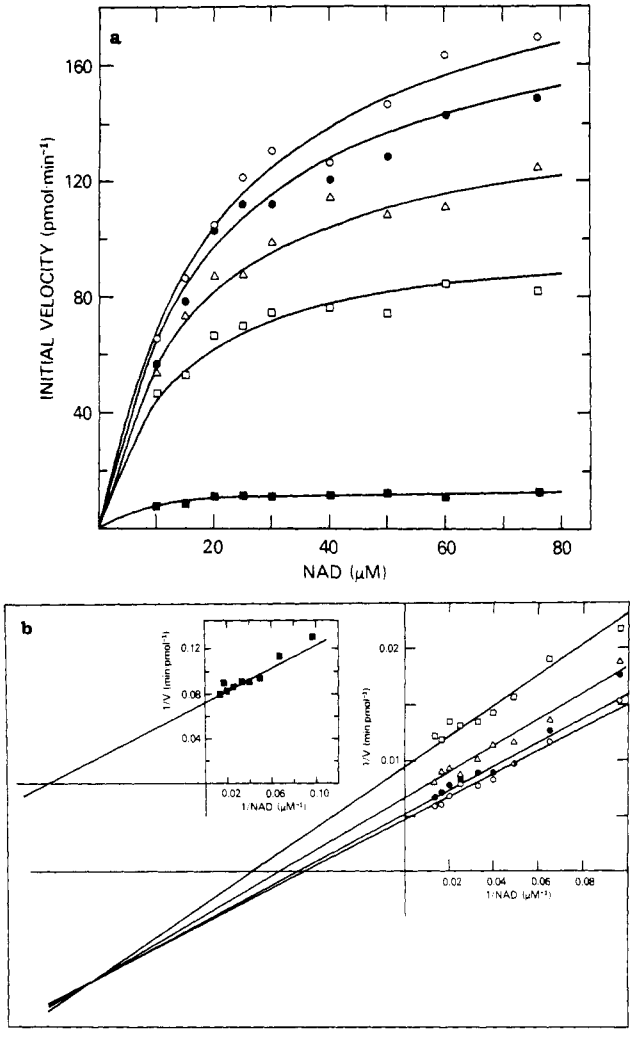

FIGURE 2: (a) Plot of initial velocity of product formation for both glycohydrolase and transferase reactions vs. NAD concentration as obtained with the erythrocyte transferase. The closed squares correspond to rates of hydrolysis of NAD. Other symbols refer to data obtained in the presence of the ADP-ribose acceptor agmatine. Concentrations of agmatine used were (□) 0.5, (△) 1, (●) 2, and (○) 3 mM. Standard assay conditions were 50 mM phosphate, pH 7.0, and 1 mg/mL ovalbumin, 30 °C, and the reaction was initiated with ET (9.1 ng/assay). A mixture of [*carbonyl*-^{14}C]NAD and [*adenine*-2,8-^{3}H]NAD was used in order to monitor hydrolysis and acceptor reaction rates in the same assay. Additional experimental details are given under Methods. The solid lines correspond to the fit of the primary V vs. [S] data to the rapid equilibrium random sequential mechanism described in the text. Data in the presence and absence of acceptor were analyzed simultaneously. (b) Double-reciprocal plot of the data in (a) obtained in the presence of agmatine. Symbols are the same as those used in (a). Inset: Double-reciprocal plot of the data in (a) obtained in the absence of acceptor. The solid lines in the main figure and inset correspond to the rapid equilibrium random sequential model described in the text.

the binding of the other substrate, and β is the ratio of maximum velocities for the glycohydrolase and transfer reactions.

The least-squares fit of the total velocity (i.e., glycohydrolase + transferase reactions) to eq 5 is given by the solid lines in Figures 1 and 2. Final kinetic parameters for both enzymes assuming a rapid equilibrium random sequential mechanism are given in Table I. With this analysis, the K_m's for NAD obtained with the glycohydrolase reaction were the same as those in the transfer reaction. The interaction parameter α was found to be greater than 1 for both enzymes. Thus, assuming equilibrium binding of substrate, each substrate increased the K_m for the other substrate. The equilibrium constants for NAD and agmatine for ET (K_A and K_B, respectively) were significantly less than the apparent K_m's observed by determining the constants in the presence of saturating second substrate.

Use of Product Inhibition To Evaluate Ordered Steady-State Mechanisms. Although the above results are inconsistent with rapid equilibrium ordered mechanisms, they cannot be

Table I: Kinetic Parameters for ADP-Ribosylation by Cholera Toxin (CT) and Erythrocyte Transferase (ET)

parameter	ADP-ribosyltransferase	
	CT	ET
K_m(NAD)	1.1 ± 0.1 mM	7 ± 0.7 μM
K_m(agmatine)	35 ± 3 mM	260 ± 20 μM
α	3.6 ± 0.3	3.8 ± 0.3
V_{max} (μmol·min^{-1}·mg^{-1})	2.8	31
β	0.02	0.05
K_I(nicotinamide) (mM)	14	0.37
γ	5.2 ± 1.3	1.2 ± 0.04

used to rule out steady-state ordered mechanisms. Equations corresponding to initial velocities for an ordered steady-state mechanism have the same general form as those used above for the random rapid equilibrium system (Segel, 1975). In many cases, these two mechanisms can be distinguished from one another with product inhibition studies. For instance, with the steady-state mechanism, the apparent inhibition constant of a product that is competitive with A and noncompetitive with respect to B would be independent of the concentration of B (the inhibitor must bind to enzyme before B, and EQB is inactive) (Segel, 1975).

The pattern for product inhibition in the random rapid equilibrium system is given below. In this case if γ, the factor

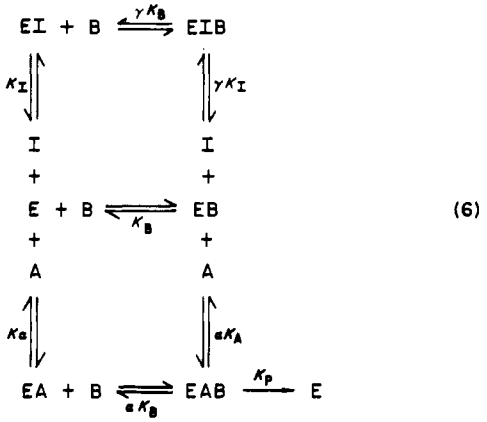

(6)

by which binding of B affects the affinity for I, is not equal to 1, then the apparent inhibition constant, K_I^{app}, changes with different fixed levels of B. The inhibition constant in the absence of acceptor was determined by measuring the hydrolysis of NAD to ADP-ribose and nicotinamide (reaction 2 above). With this value and K_A, K_B, and α from the kinetic analysis above, the only unknowns in the rapid equilibrium model are V_{max} and γ. If γ is not equal to 1, then the data are most consistent with a rapid equilibrium random sequential mechanism. If $\gamma = 1$, then kinetic data obtained by using this inhibitor cannot be used to differentiate between these two mechanisms. Inhibition by nicotinamide was evaluated at several different fixed concentrations of the acceptor agmatine. Data obtained for the transferase reaction in the presence of 50 mM agmatine for CT and 6 mM agmatine for ET are given in Figures 3 and 4, respectively. The solid lines represent the theoretical least-squares fit of the data to a rapid equilibrium random sequential mechanism using known values of K_A, K_B, K_I, and α (Table I), with V_{max} and γ as unknown variables. The best fit gave values of 5.2 and 1.2 for CT and ET, respectively. The data are thus most consistent with a random rapid equilibrium sequential mechanism rather than a steady-state ordered sequential mechanism for CT in that the apparent inhibition constant for nicotinamide depends upon the concentration of the second substrate (acceptor) agmatine. The value of γ was close to 1 for ET, and therefore, a steady-state ordered mechanism was not ruled out for ET when

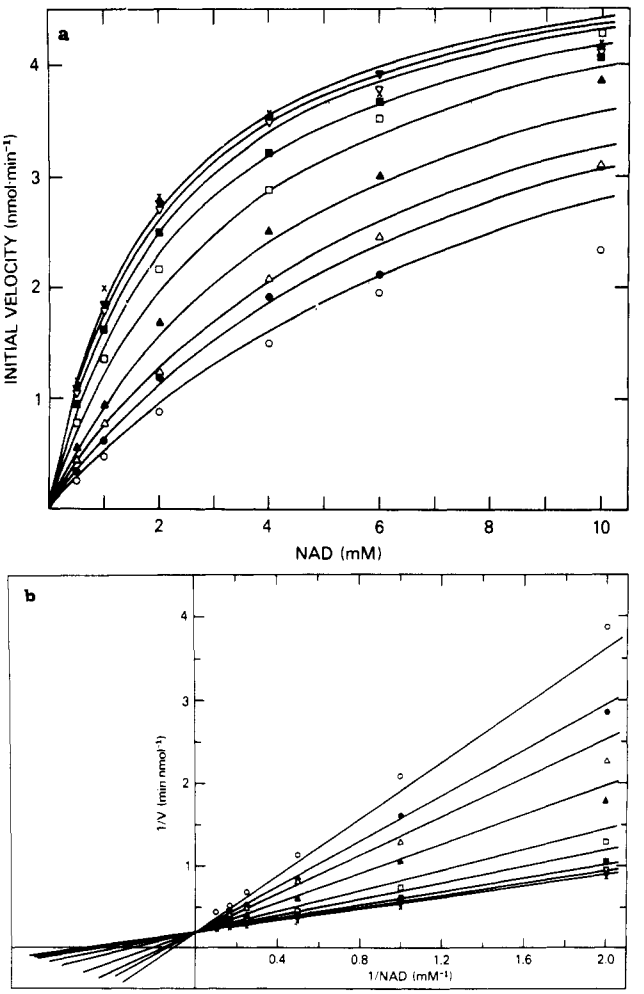

FIGURE 3: (a) Plot of the initial velocity of product formation by cholera toxin vs. NAD concentration at different fixed levels of nicotinamide and at a constant subsaturating level of the acceptor agmatine. Concentrations of nicotinamide were (▼) 2, (▽) 4, (■) 10, (□) 20, (▲) 40, (△) 60, (●) 75, and (○) 100 mM. The crosses correspond to data obtained in the absence of inhibitor. The concentration of agmatine was 50 mM. Reactions were performed at 30 °C in buffer containing 400 mM potassium phosphate (pH 7.0), 20 mM dithiothreitol, 1 mg/mL ovalbumin, and [*adenine*-U-^{14}C]NAD and were initiated by addition of enzyme. The solid lines correspond to the fit of the data to the theoretical rapid equilibrium sequential model in the presence of a competitive inhibitor. Details are given in the text. (b) Double-reciprocal plot of the data in (a). Symbols and solid lines have the same meaning as given in (a).

agmatine was used as the ADP-ribose acceptor.

Discussion

The findings in the present report support a rapid equilibrium model for the avian NAD:arginine ADP-ribosyltransferase and the enzymatically active subunit of cholera toxin (eq 4 above). In this model, A and B correspond to NAD and agmatine, respectively, and the equilibrium dissociation constants are given by K_A and K_B, respectively. The factor β is equal to the ratio of maximal velocities of the glycohydrolase and transferase reactions. To obtain accurate estimates of the kinetic parameters, glycohydrolase and transferase reactions were measured simultaneously by using appropriate tracers in the same assay. Both NAD and ADP-ribose acceptors bind randomly to the transferase; binding of either NAD or agmatine has a negative effect on the subsequent binding of the other substrate, resulting in fixed substrate-dependent Michaelis constants for the variable substrate. This mechanism for CT differs from one proposed earlier which postulated an ordered sequential mechanism in which

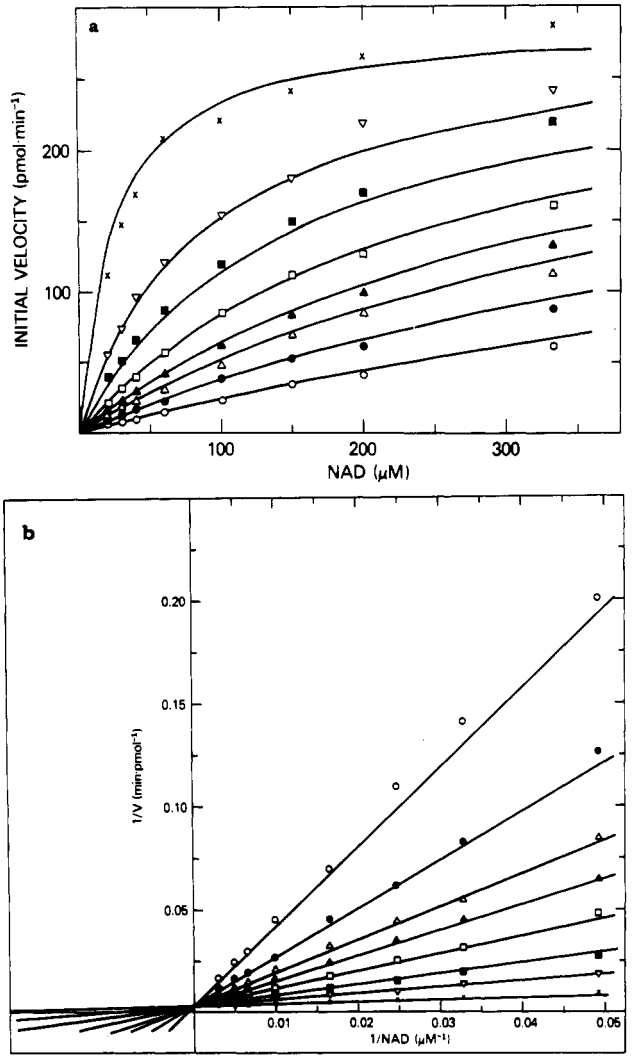

FIGURE 4: (a) Plot of the initial velocity of product formation vs. NAD concentration as obtained by using erythrocyte transferase at several different concentrations of nicotinamide and a subsaturating level of the acceptor agmatine (6 mM). The concentrations of nicotinamide used were (▽) 1.2, (■) 2.4, (□) 4, (▲) 6, (△) 8, (●) 12, and (○) 20 mM. The crosses correspond to data obtained in the absence of inhibitor. The assay conditions were 50 mM potassium phosphate, pH 7.0, and 1 mg/mL ovalbumin, 30 °C, and were initiated by ET. [*adenine*-U-^{14}C]NAD was used as a tracer to monitor reaction velocities. The solid lines correspond to the fit of the data to the rapid equilibrium random sequential model in the presence of a competitive inhibitor described in the text. (b) Double-reciprocal plot of the data in (a). Symbols and solid lines are the same as those in (a).

the first substrate to bind was NAD (Mekalanos et al., 1979). The present studies are consistent with the hypothesis that, under our assay conditions using agmatine as the ADP-ribose acceptor, the substrates can bind to CT in random order.

The observation that binding of one substrate lowered the affinity for the second substrate led us to believe that we might be able to differentiate kinetically between rapid equilibrium random and steady-state ordered mechanisms by product inhibition studies. If binding of the competitive inhibitor nicotinamide changed the affinity for agmatine and vice versa, as was found for NAD and agmatine, then the system could be described by using an inhibitor interaction parameter, γ, and a substrate interaction parameter, α. If $\gamma \neq 1$, then the apparent inhibition constant would vary with agmatine concentration. For ET, γ was close to 1, and therefore, kinetic studies with nicotinamide could not be used to differentiate between rapid equilibrium random and steady-state ordered mechanisms. The inhibitor interaction parameter for CT, 5.2, indicated that the binding of the acceptor agmatine decreased the affinity for nicotinamide by approximately half an order of magnitude. The combined results for CT were thus most consistent with a random rapid equilibrium mechanism in that the apparent inhibition constant for nicotinamide increased with increasing concentrations of agmatine.

Under the framework of the rapid equilibrium mechanism, one obtains the equilibrium constant for interaction of either substrate with the free enzyme as well as the factor by which binding of one substrate changes the affinity for the second substrate. This factor, α, must be the same for both substrates, since this model assumes rapid equilibrium binding of both substrates and changes in free energy must be independent of path (see above model). For ET and CT, α was found to be approximately 3.5 with agmatine as the acceptor, and therefore, binding of NAD or agmatine results in a greater than 70% decrease in the affinity for the second substrate. Conceivably, in the presence of the physiological acceptor, which has not yet been identified, α may differ from the value found for agmatine. To some extent, variation in α may enhance substrate specificity such that certain arginine residues or guanidino compounds are more readily ADP-ribosylated. Although CT appears to be able to use a variety of proteins and guanidino compounds in vitro (Moss & Vaughan, 1981), in intact cells, it appears that toxin preferentially ADP-ribosylates two membrane proteins of 42 and 47 kilodaltons (Moss & Vaughan, 1978, 1981; Cassel & Pfeuffer, 1978; Gill & Meren, 1978; Johnson et al., 1978; Watkins et al., 1981). Current studies are directed at determining whether α may be critical to the regulation of the rates of ADP-ribosylation of potential acceptor substrates.

ACKNOWLEDGMENTS

We thank D. Marie Sherwood and Barbara Ziarnik for expert secretarial assistance and Dr. Martha Vaughan for critical review of the manuscript.

Registry No. NAD, 53-84-9; agmatine, 306-60-5; nicotinamide, 98-92-0; NAD:arginine ADP-ribosyltransferase, 81457-93-4; NAD:protein ADP-ribosyltransferase, 58319-92-9.

REFERENCES

Burzio, L. O., Riquelme, P. T., & Koide, S. S. (1979) *J. Biol. Chem. 254*, 3029–3037.

Cassel, D., & Pfeuffer, T. (1978) *Proc. Natl. Acad. Sci. U.S.A. 75*, 2669–2673.

Chung, D. W., & Collier, R. J. (1977) *Biochim. Biophys. Acta 483*, 248–257.

Ferro, A. M., & Oppenheimer, N. J. (1978) *Proc. Natl. Acad. Sci. U.S.A. 75*, 809–813.

Gill, D. M., & Meren, R. (1978) *Proc. Natl. Acad. Sci. U.S.A. 75*, 3050–3054.

Goff, C. G. (1974) *J. Biol. Chem. 249*, 6181–6190.

Hayaishi, O., & Ueda, K. (1977) *Annu. Rev. Biochem. 46*, 95–116.

Johnson, G. L., Kaslow, H. R., & Bourne, H. R. (1978) *J. Biol. Chem. 253*, 7120–7123.

Kandel, J., Collier, R. J., & Chung, D. W. (1974) *J. Biol. Chem. 249*, 2088–2097.

Katada, T., Tamura, M., & Ui, M. (1983) *Arch. Biochem. Biophys. 224*, 290–298.

Lowry, O. H., Rosebrough, N. J., Farr, A. L., & Randall, R. J. (1951) *J. Biol. Chem. 193*, 265–275.

Manning, D. R., Fraser, B. A., Kahn, R. A., & Gilman, A. G. (1984) *J. Biol. Chem. 259*, 749–756.

Mekalanos, J. J., Collier, R. J., & Romig, W. R. (1979) *J. Biol. Chem. 254*, 5849–5854.

Moss, J., & Vaughan, M. (1977) *J. Biol. Chem. 252*, 2455–2457.
Moss, J., & Richardson, S. H. (1978) *J. Clin. Invest. 62*, 281–285.
Moss, J., & Vaughan, M. (1978) *Proc. Natl. Acad. Sci. U.S.A. 75*, 3621–3624.
Moss, J., & Stanley, S. J. (1981) *Proc. Natl. Acad. Sci. U.S.A. 78*, 4809–4812.
Moss, J., & Vaughan, M. (1981) *Mol. Cell. Biochem. 37*, 75–90.
Moss, J., Manganiello, V. C., & Vaughan, M. (1976) *Proc. Natl. Acad. Sci. U.S.A. 73*, 4424–4427.
Moss, J., Garrison, S., Oppenheimer, N. J., & Richardson, S. H. (1979a) *J. Biol. Chem. 254*, 6270–6272.
Moss, J., Stanley, S. J., & Oppenheimer, N. J. (1979b) *J. Biol. Chem. 254*, 8891–8894.
Moss, J., Stanley, S. J., & Watkins, P. A. (1980) *J. Biol. Chem. 255*, 5838–5840.
Moss, J., Stanley, S. J., Burns, D. L., Hsia, J. A., Yost, D. A., Myers, G. A., & Hewlett, E. L. (1983) *J. Biol. Chem. 258*, 11879–11882.
Ogata, N., Ueda, K., & Hayaishi, O. (1980a) *J. Biol. Chem. 255*, 7610–7615.
Ogata, N., Ueda, K., Kagamiyama, H., & Hayaishi, O. (1980b) *J. Biol. Chem. 255*, 7616–7620.
Oppenheimer, N. J. (1978) *J. Biol. Chem. 253*, 4907–4910.
Oppenheimer, N. J., & Bodley, J. W. (1981) *J. Biol. Chem. 256*, 8579–8581.
Pappenheimer, A. M., Jr. (1977) *Annu. Rev. Biochem. 46*, 69–94.
Pekala, P. H., & Moss, J. (1983) *Curr. Top. Cell. Regul. 22*, 1–49.
Riquelme, P. T., Burzio, L. O., & Koide, S. S. (1979) *J. Biol. Chem. 254*, 3018–3028.
Segel, J. H. (1975) *Enzyme Kinetics*, pp 273–330, Wiley, New York.
Ueda, K., Okayama, H., Fukushima, M., & Hayaishi, O. (1975) *J. Biochem. (Tokyo) 77*, 1p.
Van Ness, B. G., Howard, J. B., & Bodley, J. W. (1980a) *J. Biol. Chem. 255*, 10710–10716.
Van Ness, B. G., Howard, J. B., & Bodley, J. W. (1980b) *J. Biol. Chem. 255*, 10717–10720.
Vaughan, M., & Moss, J. (1981) *Curr. Top. Cell. Regul. 20*, 205–246.
Watkins, P. A., Moss, J., & Vaughan, M. (1981) *J. Biol. Chem. 256*, 4895–4899.

Small-Angle Neutron Scattering Study of Lateral Phase Separation in Dimyristoylphosphatidylcholine–Cholesterol Mixed Membranes†

W. Knoll,* G. Schmidt, K. Ibel,‡ and E. Sackmann
Physik Department E22, Biophysics Group, Technical University of Munich, D-8046 Garching, FRG
Received December 26, 1984

ABSTRACT: The small-angle neutron scattering (SANS) technique developed previously is used to study the lateral phase separation in dimyristoylphosphatidylcholine (DMPC)–cholesterol mixed vesicles in the L_α (35 °C) and $L_{\beta'}$ (7 °C) phase of DMPC. To increase the sensitivity of the previous method, we apply the so-called inverse contrast variation technique where contrast matching is performed at a constant H_2O/D_2O ratio by varying the ratio of DMPC with deuterated and protonated hydrocarbon chains. Phase boundaries can be determined to an accuracy of ±0.5 mol %. In parallel experiments phase separation in the $L_{\beta'}$ phase was also studied by freeze–fracture electron microscopy. For DMPC in the L_α phase complete miscibility is clearly established up to cholesterol molar fractions of $x_c = 0.14$. Strong evidence is provided that this is also the case up to $x_c \approx 0.45$. Cholesterol is no longer soluble above this limit and precipitates as small crystallites. For the $L_{\beta'}$ phase (7 °C) phase boundaries are clearly established at $x_{c1} = 0.08$ and $x_{c2} = 0.24$, and very strong evidence is provided for two additional boundaries at $x_{c3} = 0.435$ and $x_{c4} \approx 1.0$. At $0 \leq x_c \leq x_{c1}$ the mixture forms a tilted solid solution in both the $L_{\beta'}$ and $P_{\beta'}$ phase while at $x_{c1} \leq x_c \leq x_{c2}$ this phase coexists with a nontilted mixture containing 24 mol % cholesterol. At $x_{c2} \leq x_c \leq x_{c3}$ a second region exists where mixtures containing 24 and 43.5 mol % cholesterol coexist within the plane of the membrane. To fulfill the phase rule, x_{c2} must correspond to a stoichiometric mixture which would reconcile the concepts of phase separation and complex formation. Our freeze–fracture studies do not provide evidence for a decrease of the repeat distance of the ripple phase at $x_c \leq 0.08$ and for a regular ripple phase with defined ripple distance within the first coexistence region.

Since cholesterol is a major component of plasma membranes, its interaction with phospholipids in particular synthetic lecithins has been studied extensively in bilayers and monolayers (Albrecht et al., 1981; Cadenhead & Müller-Landau, 1984). A variety of methods has been applied including calorimetry (Mabrey et al., 1978; Estep et al., 1978), densitometry (Melchior et al., 1980), X-ray or electron diffraction (Hui & He, 1983), and spectroscopic techniques (Recktenwald & McConnell, 1981).

Despite this wealth of experimental data the thermodynamic and structural properties of the cholesterol–lecithin mixture

† This work was supported by the Bundesministerium für Forschung und Technologie.
‡ Permanent address: Institut Laue-Langevin, 156 × Centre de Tri, F-38042 Grenoble Cedex, France.

0006-2960/85/0424-5240$01.50/0